Journal of Theoretical and Applied Physics (2020) 14:315–321
https://doi.org/10.1007/s40094-020-00388-z

RESEARCH

# Enhancement of charge breeding efficiency for rare isotope beam with the control of magnetic field profile and electron beam energy in EBIS

**J. W. Kim**[1]

Received: 19 December 2019 / Accepted: 8 August 2020 / Published online: 13 August 2020


**Abstract**
The magnetic field in the ion trap of electron beam ion source (EBIS) determines the current density of electron beam and thus the depth of trap potential, which affects the charge breeding efficiency to desired charge state. An EBIS charge breeder has been constructed to be used for the Rare Isotope Science Project in Korea. A 6 T superconducting solenoid is used for the trap, and uniform magnetic field is extended with correction coils at the ends. The effect of field uniformity on the electron current density is evaluated using TRAK, and it is shown sizable improvement in the charge breeding efficiency for rare isotope beams can be obtained by elaborate magnetic design. Furthermore, the electron beam energy affects the ionization efficiency. The electron energy is often reduced in the trap for optimal matching with charge striping cross section. However, virtual cathode formation can appear in the process of energy reduction. Maximum beam currents limited by electron energy are studied analytically and by TRAK simulation in the view of improving the charge breeding efficiency.

**Keywords** Electron beam ion source (EBIS) · Superconducting magnet · Charge breeding · Rare isotope beam · Virtual cathode

## Introduction

Production of high-current and high-quality beams of highly charged ions from ion source is an important consideration for the efficient operation of high-intensity heavy-ion accelerator facility. An electron beam ion source (EBIS) can provide highly charged pulsed beams for synchrotron and linear accelerator, and is well suited for charge breeding of rare isotope beams for reacceleration [1].

An EBIS has been constructed for Rare Isotope Science Project (RISP) in Korea as a charge breeder of isotopes produced by isotope separation on-line (ISOL) method [2, 3]. The isotopes will be charge-bred to have the A/q below 7 for the injection into a superconducting (SC) linac. The EBIS will be operated in a pulsed injection mode with the use of a radio frequency quadrupole cooler buncher (RFQ-CB) located upstream of the EBIS [4]. The EBIS is under preparation for off-line test as shown in Fig. 1 prior to the final installation in the new ISOL facility in the end of 2020. A Cs surface ion source will be used in the test, and charge-bred beams will be analyzed using a time-of-flight measurement system similar to the one used at Brookhaven National Laboratory [5].

Charge breeding efficiency to desired charge state is a key parameter in planning physics program using rare isotope beams. A major requirement is to breed $Cs^{1+}$ into $Cs^{27+}$ with an efficiency of over 20%. While the structural design of this EBIS is based on that for CARIBU at Argonne National Laboratory [6], the SC-solenoid for ion trapping is designed to have an extended uniform field region. The ion beam current reaching the charge state of interest depends on ionization factor, which is the product of electron current density and confinement time. Maximum current of the electron gun is increased from 2 to 3 A for RISP.

The major parameters of EBIS for RISP and for CARIBU are compared in Table 1. The cathode is made of IrCe with a diameter of 5.6 mm, which was manufactured by Budker Institute for Nuclear Physics (BINP). BINP also provided the cathode package including the electron gun coil. The gun was first tested by pulsing the anode voltage, while

✉ J. W. Kim
jwkim@ibs.re.kr

[1] Rare Isotope Science Project, Institute for Basic Science, Daejeon 34000, Korea

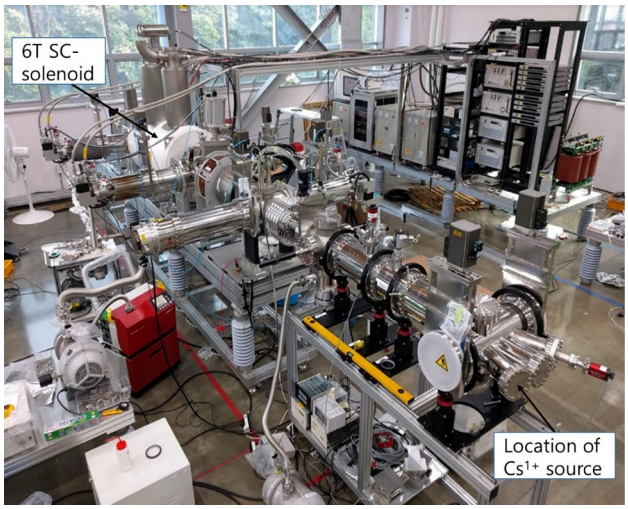


**Fig. 1** The EBIS system under preparation for off-line test using a $Cs^{1+}$ source

**Table 1** Comparison of major EBIS parameters for RISP and CARIBU

| | RISP | CARIBU |
|---|---|---|
| $B_{max}$ | 6 T | 6 T |
| $I_{max}$ | 3 A | 2 A |
| Dia. of cathode | 5.6 mm | 4 mm |
| Trap length | 76 cm | 70 cm |
| Tube diameter | 24 mm | 20 mm |
| Warm bore diameter | 203 mm | 155 mm |
| $J_{max}$ of election beam | 500 A/cm$^2$ | 500 A/cm$^2$ |
| Election energy of gun/in trap | 20 keV/12 keV | 10 keV/4–5 keV |

extracted electrons being dumped to the anode [3]. At a test bench in 2019 including both the gun and electron collector, the current reached up to around 2 A. The warm bore tube contains normal conducting coils for orbit correction and getter pumps for ultra-high vacuum. This bore diameter is increased from that of CARIBU to improve vacuum in the long trap and to reduce ion contaminants for higher efficiency of charge breeding.

Ion trapping by space charge of the electron beam can be improved with uniform electron current density, i.e., uniform magnetic field in the trap. When the magnetic field varies, the radial potential well is changed. This variation leads to larger amplitude of ion radial motion, and thus, ions can leave the electron beam boundary to spend time outside of the beam. This effect can result in broadening the charge state distribution compared to the model of 100% ion–electron overlap. We used TRAK [7] to calculate electron trajectories self-consistently by accounting for electron beam's space charge.

The ionization cross section is typically a maximum when electron energy is near ionization potential. The drift tube voltages can be controlled to vary the beam energy for higher charge breeding efficiency. However, virtual cathode effect can occur in the trap when the beam energy is reduced below the threshold energy for given electron current. Analytic approximation and TRAK simulation were performed to evaluate the current limitation due to the virtual cathode effect, which aims to guide EBIS operation.

## Extended uniform magnetic field of 6 T SC-solenoid

The maximum magnetic field in the trap is set to be 6 T considering the breeding time required for rare isotope beams and the availability of reliable SC-magnet with a warm bore size of 203 mm. A 6 T SC-magnet was built by Tesla Engineering Ltd., and its major parameters are listed in Table 2. To extend uniform field region, two coils are added at the ends of the solenoid, which lowers the field intensity at the center. The added coils are serially connected to the solenoid with ultra-low resistance. The magnet operates in persistent mode to keep the field highly stable. Variation of the magnetic field is measured using a Gauss meter to be less than 0.1 ppm after finishing current ramping and further decreases after 30 h or so.

The magnetic field was mapped along the axis first at the factory and checked at the site using a Hall probe, which was guided by an aluminum tube as shown in Fig. 2. The field profile at 6 T is given in Fig. 3 showing that its uniformity meets the requirement. The central axis of solenoidal field was searched by measuring the axial fields around a fixed distance from the mechanical center. The Hall probe was located near the two ends of the cryostat, where the gradient of axial field is large, allowing for high sensitivity of this centering method. The magnetic axis was determined by decreasing differences in the fields of opposite angular locations. Finally, the end flanges for the beam tube, which are designed to be adjustable by 5 mm in transverse directions, are fixed to the field center. Some details of the field mapping device are shown in Fig. 2.

**Table 2** Major parameters of the 6 T magnet

| Parameter | Values |
|---|---|
| $B_{max}$ | > 6 T at center |
| $I_{op}$ at 6 T | 96.2 A |
| Inductance | 280.9 H |
| Stability | < 0.1 ppm/h |
| Uniformity (length) | < ±0.4% (< ±35 cm) |
| | < ±4% (< ±40 cm) |


**Fig. 2** The 6 T SC-solenoid placed on the support frame and a mapper guide installed for field mapping. The support structure of Hall probe is made of glass fiber composite and four adjustable blocks to locate end flanges are attached to the cryostat

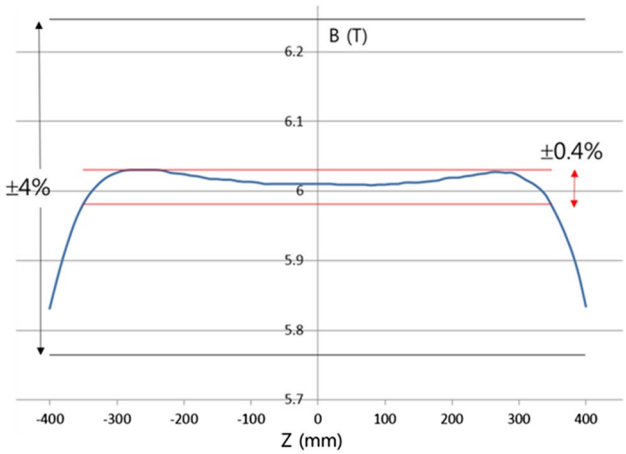


**Fig. 3** The magnetic field measured along the axis with the boundaries of field uniformity indicated

A larger total charge capacity can be obtained with a longer trap [8], which is suitable for charge breeding of abundant stable ions. However, to increase the efficiency of charge breeding to desired charge, a longer and uniform magnetic field can be more effective. The effects of uniform magnetic field on electron current density are studied with and without compensation coils as shown in Fig. 4. Figure 4 also shows the profiles of magnetic fields calculated by TRAK along the axis. The solenoid does not use ferromagnetic yoke to confine the magnetic flux, so that the range of fringe field is quite long. The region of 100 G lines is about 3 m away in the perpendicular direction from the axial center of the 6 T magnet. In fact, this large stray field affects the operation of nearby components. Moving parts of vacuum pumps should be locally shielded. The use of iron shields in the cryostat of the SC-solenoid can be also feasible with some care not to disturb cylindrical symmetry as has been considered in CERN [9].

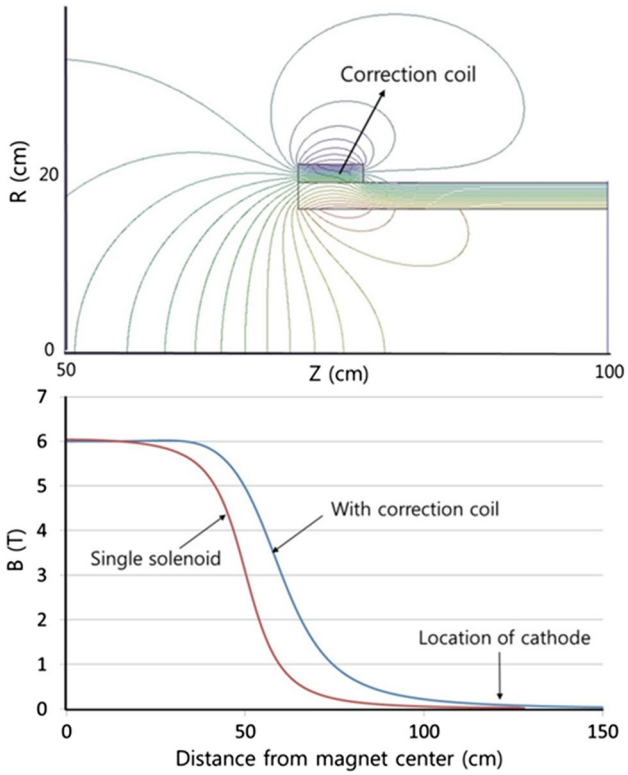


**Fig. 4** Upper: Configuration of the solenoid with correction coil. Lower: The axial magnetic fields of the two cases

Axial magnetic field profiles in the cathode are plotted in Fig. 5, which shows the correction coil increases stray fields in the axial direction. The higher fringe field is helpful for the electron gun to be immersed in the field with the gun coil field strength reduced. Also, magnetic mirror effects, which may occur between the gun coil and SC-magnet such as in case 2 of Fig, 5, can be avoided.

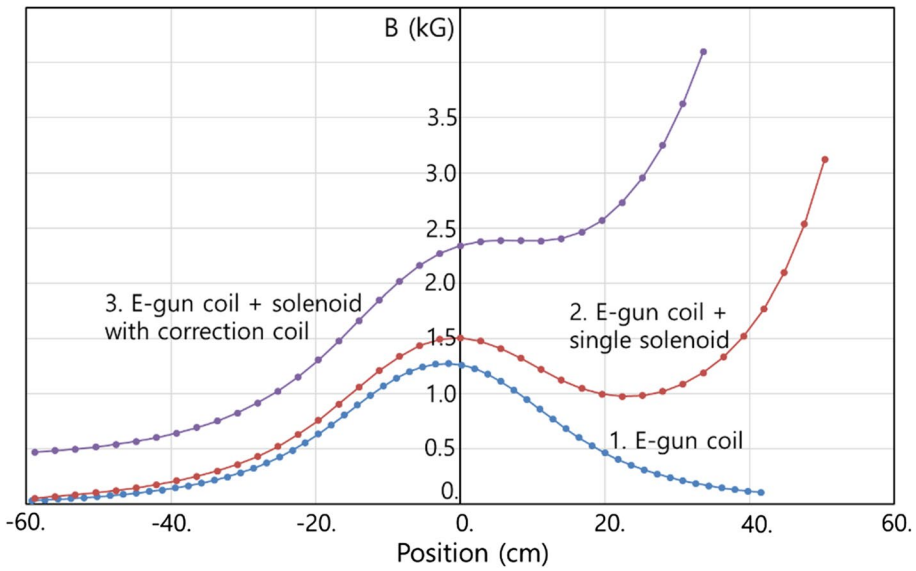


**Fig. 5** Axial magnetic field profiles on axis in the electron gun, where the fringe field of the 6 T solenoid helps immersing the electron beam. The cathode's emission surface is at zero, and the anode tube is at 7.8 cm

## Simulation study of electron current density using TRAK

The electron beam optics is simulated using TRAK. The magnetic and electric fields are assumed to be cylindrically symmetric. Iterations of particle tracking followed by updates of the electric field solution are performed until the final electron kinetic energies converge. The cathode surface has a convex shape to make the electron beam flow more laminar. When the beam energy is reduced in the trap, the laminar flow may help in lessening electron losses on other than electron collector [10]. The full envelope of electron beam in the EBIS is given in Fig. 6 along with the locations of drift tubes [11]. At the collector, the electron beam is strongly defocused with the use of soft iron cover to shield the stray field of the 6 T magnet, and an electrostatic repeller is used to reflect the beam.

Sectional electron densities at the five locations indicated in Fig. 6 are calculated with TRAK and plotted in Fig. 7 for the two cases of magnetic field profiles. Much larger variation of current densities appears in the case of without corrective coil as predicted by magnetic compression of the immersed cathode:

$$j(z) = j_c \frac{B(z)}{B_c},$$

where $j_c$ and $B_c$ are the electron current density and the magnetic field intensity at the cathode, respectively.

The current density profiles along the trap are plotted in Fig. 8, where the density is an average on the plateau of Fig. 7, reflecting the variation of magnetic fields. The field intensity on the cathode is kept at 1.9 kG in TRAK simulation. For a given length of the magnet, the trap length can be further increased by adding doubly stacked coils instead of single layer. The effect of field oscillation on charge breeding efficiency to desired charge state could be perhaps evaluated by simulation tools like EBIS-PIC [12] in the future.

The maximum positive charge capacity that is trapped in the electron beam can be estimated with:

$$Q = 3.3 \times 10^{11} f L I_e E^{-1/2}$$

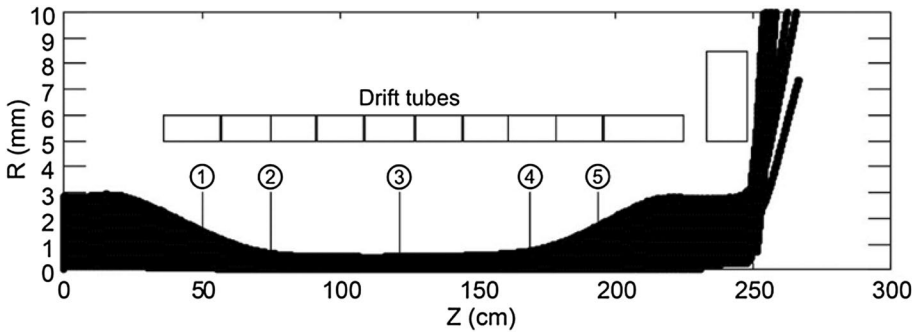


**Fig. 6** Electron beam envelope from cathode to collector. Five locations are indicated, where the electron beam profiles are plotted in Fig. 7

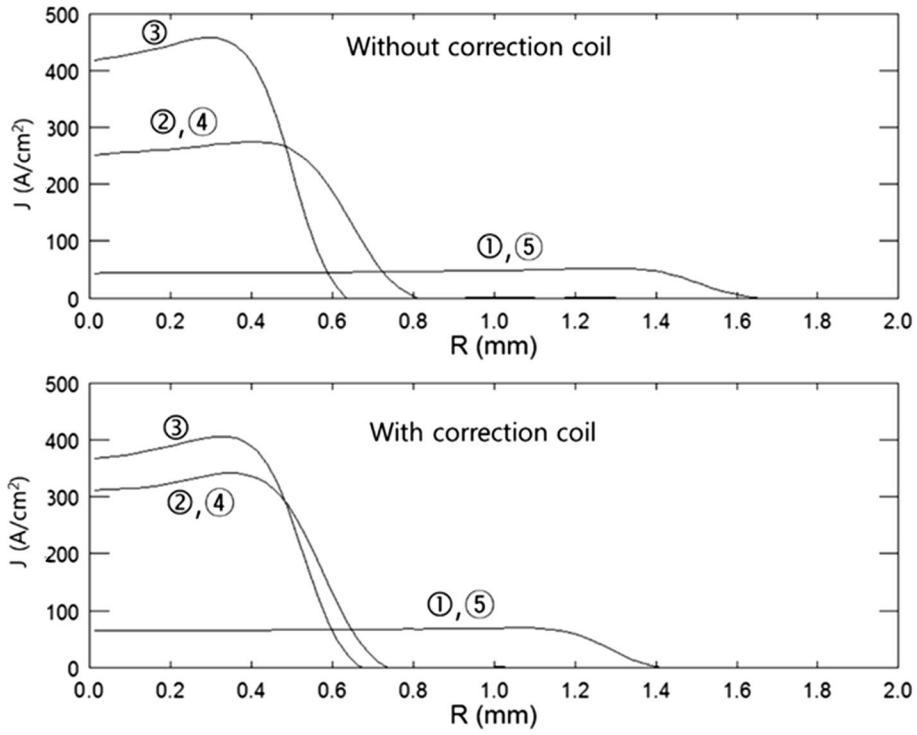


**Fig. 7** Current density profiles at the locations noted in Fig. 6 for the two profiles of magnetic fields. The plateau is defined to the radius, where $J$ is the same as that at the center

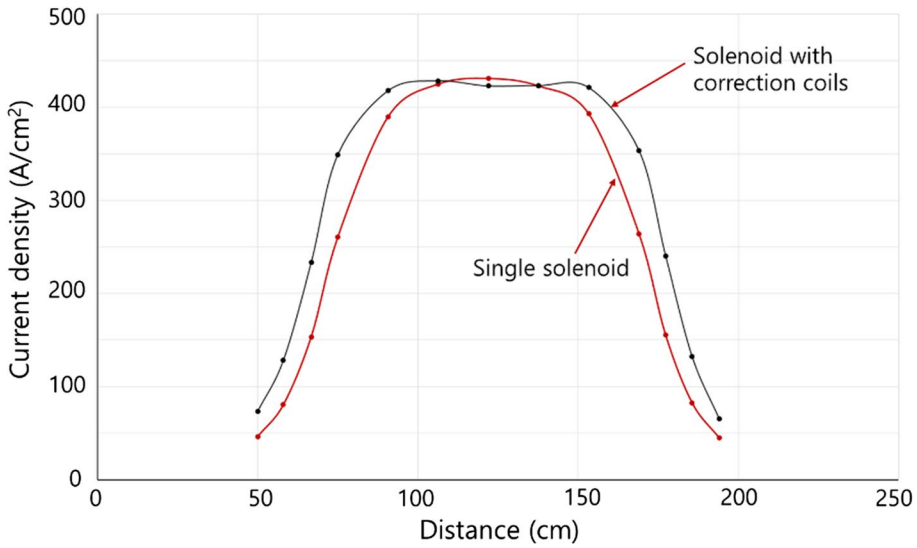


**Fig. 8** Current density profiles in the trap region for the two profiles of magnetic fields

where $f$ is electron beam neutralization factor with a value of around 0.5–0.7, $L$ is the length of the trap in m, $I_e$ is the electron current in A, and $E$ is the electron beam energy in keV. Provided with an electron beam of 3 A at an energy of 10 kV in the ion trap length of 0.76 m, the charge capacity is around $1.43 \times 10^{11}$ if assuming $f$ is 0.6, which is acceptable for most of rare isotopes expected from RISP.

The extended uniform field increases the positive charge capacity proportionally, and uniform electron current density will enhance the efficiency of charge breeding to desired single charge state by reducing radial oscillation of trapped ions.

## Virtual cathode formation in the trap

The electron beam energy is another parameter affecting the breeding efficiency to desired charge state. If the energy is much higher than ionization potentials in the trap, the efficiency can be improved by lowering electron energy with the

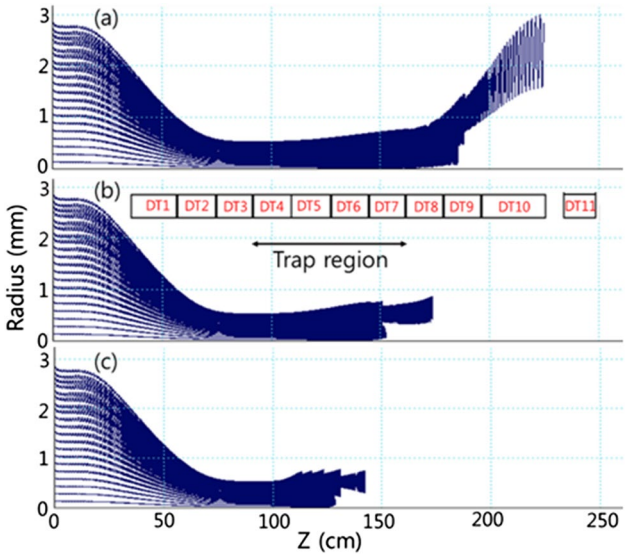


**Fig. 9** Electron beam trajectories when the four drift tubes in the trap region are kept at the voltages of: 4.5 kV (**a**), 4 kV (**b**), 3.5 kV (**c**). The bias voltage on the cathode is −4 kV

control of drift tube voltages. However, deceleration of the electron beam can cause forming virtual cathode. A virtual cathode is often formed by halo electron beam and reflects electrons back to the cathode or to the wall of drift tubes, which is characterized by complex non-stationary dynamics [13].

The electron current for virtual cathode formation can be estimated as below when the beam is not space charge compensated [14]:

$$I_B(A) = 25.4 \times 10^{-6} \frac{V_0^{3/2}(V)}{1 + 2\ln(r_t/r_e)}$$

where $r_t$ is the inner radius of drift tube, $r_e$ is the radius of electron beam, and $V_0$ is the potential difference between the electron cathode and the drift tube. With the radii of the tube and the electron beam fixed to 24 mm and 0.5 mm, respectively, $I_B$ is determined by the electron beam energy in the trap. $I_B$ is around 3 A when the electron energy is 7 keV.

TRAK simulations are performed to investigate the formation of virtual cathode. Figure 9 shows the reversed electron flow due to space charge when the voltage applied to four drift tubes in the trap region is decreased from 4.5 to 4 and then to 3.5 kV. The cathode voltage is biased at −4 kV, and the anode voltage is 16 kV. The virtual cathode effect strongly appears at an electron energy of 8 keV for a current of 3 A. This TRAK result roughly agrees with the estimate of 7 keV previously performed using the analytic formula.

As listed in Table 1, a typical electron energy in the trap is 12 kV, which is above threshold energy of virtual cathode formation. However, further energy reduction for some isotopes to enhance the charge breeding efficiency will be limited especially considering possible onset of the effect at higher electron energies due to non-ideal environment.

## Conclusions

The charge-bred beam current to desired charge state can be improved with an elaborate design of magnetic field in the trap. The 6 T solenoid for RISP is designed to have an extended uniform field region for ion trapping compared to that for CARIBU. TRAK simulations show the electron current density is more uniform in a wider range. In addition, the higher stray field by correction coil is useful because smaller electron gun coil current can be used to immerse the cathode, also avoiding any magnetic mirror effect between the gun coil and SC-solenoid. In the future, multilayer correction coils could be considered to shape the trap field, while advanced charge breeding calculation in 3D guiding to optimize the field profile.

Electron beam energy in the trap is a major parameter affecting ionization efficiency, but virtual cathode formation can occur due to space charge when the electron energy is reduced. Depending on nuclei in the trap, electron beam energy can be adjusted considering both charge breeding efficiency and virtual cathode effect. Practical operation parameters of the EBIS can be studied when the beam operation starts in 2021.

**Acknowledgements** The author would like to thank Mr. S. J. Heo and Drs. H. J. Son, Y. H. Park and T. S. Shin of the Institute for Basic Science for their helps in magnetic field measurement. This work is supported by the Ministry of Science, ICT and Future Planning (MSIP) and Technology and the National Research Foundation (NRF) of the Republic of Korea under Contract 2013MA1A1075764.

## References

1. Wenander, F.: Charge breeding of radioactive ions with EBIS and EBIT. J. Instrum. **5**, C10004 (2010)
2. Park, Y., Son, H., Kim, J.: Design of an EBIS charge breeder system for rare-isotope beams. J. Korean Phys. Soc. **69**, 962–966 (2016)
3. Son, H., Park, Y., Kondrashev, S., Kim, J., Kim, B., Chung, M.: Development of an EBIS charge breeder for the Rare Isotope Science project. Nucl. Instrum. Methods B **408**, 334–338 (2017)
4. Boussaid, R., Park, Y., Kondrashev, S.: Technical design of RISP RFQ cooler buncher. J. Korean Phys. Soc. **71**, 848–854 (2017)
5. Alessi, J., Beebe, E., Hershcovitch, A., Kponou, A., Prelec, K.: Progress in the BNL program for a RICH EBIS. Proc. of EPAC1996, pp. 1463–1465 (1996)
6. Ostroumov, P., Barcikowski, A., Dickerson, C., Mustapha, B., Perry, A., Sharamentov, S., Vondrasek, R., Zinkaan, G.: Off-line commissioning of EBIS and plans for its integration into ATLAS and CARIBU. Rev. Sci. Instrum. **87**, 02B506 (2016)
7. See http://www.fieldp.com/ for Finite-element Software for Electromagnetics

8. Pikin, A., Alessi, J., Beebe, E., Okamura, M., Raparia, D., Ritter, J., Snydstrup, L.: TANDEM EBIS Proc. of 12th HIAT, pp. 101–104 (2012)
9. Breitenfeldt, M., Mertzig, R., Pitters, J., Shornikov, A., Wenander, F.: The twin EBIS setup: machine description. Nucl. Instrum. Methods A **856**, 139–146 (2017)
10. Kalinin, Y., Hramov, A.: Experimental and theoretical investigation into the effect of the electron velocity distribution on chaotic oscillations in an electron beam under virtual cathode formation conditions. Tech. Phys. **51**, 558–566 (2006)
11. Kondrashev, S., Kim, J., Park, Y., Son, H.: Advanced EBIS charge breeder for Rare Isotope Science Project. Proc. of IPAC2016, pp. 1304–1307 (2016)
12. Zhao, L., Kim, J.S.: Simulation of ion beam injection and extraction in an EBIS. Rev. Sci. Instrum. **87**, 02A908 (2016)
13. Kurkin, S., Badarin, A., Koronivskii, A., Hramov, A.: The development and interaction of instabilities in intense relativistic electron beam. Phys. Plasma **22**, 122110 (2015)
14. Nezlin, M.: Physics of Intense Beams in Plasmas. Institute of Physics Publishing, Bristol (1993)